Experiments for collection and characterization of particles exiting from solid propellant rocket nozzles

F. Maggi* and S. Carlotti.†
Politecnico di Milano, Milano, Italy, 20156

D. Saile‡ and A. Gülhan.§
German Aerospace Center (DLR), Cologne, Germany, 51147

M. Liljedahl¶ and N. Wingborg.‖
Swedish Defence Research Agency (FOI), Tumba, Sweden, SE-147

T. Langener** and J. Van den Eynde.††
European Space Agency (ESA-ESTEC), Noordwjik, The Netherlands, 2200AG

Metals in solid propellants are used to improve specific impulse and increment the energy density. Their combustion generates condensed products that move along the motor chamber and are expelled through the nozzle. The discharge of liquid or solid particles across the gas dynamic nozzle of large boosters is not only a matter of specific impulse loss. Recent climatological studies are addressing possible short and long term environmental effects that may be attributed to space launch activity by large launchers. In this respect, the knowledge of plume content and, specifically, of physical, chemical, and morphological properties of the exhausted particulate is needed. In the frame of the EMAP (Experimental Modelling of Alumina Particulate in Solid Booster) project, an activity financed by the European Space Agency, the Space Propulsion Laboratory (SPLab) of Politecnico di Milano developed a collection method and an analysis protocol for the characterization of the particles contained in the rocket plume. The collection is performed by an intrusive probe capable of capturing the particles directly from the nozzle exit and quenching them. The post-collection protocol enables size measurement, chemical characterization, and morphology observation. In this paper an overview of the collection and analysis activity is presented, along with the final results that were achieved by analyzing the plume of different rocket motors.

I. Nomenclature

$D(3,2)$	=	surface-mean diameter
$D(4,3)$	=	volume-mean diameter
$d(0.x)$	=	diameter at the given percentile
p_{cc}	=	chamber pressure

II. Introduction

An AGARD workshop in 1995 addressed the global environmental impact of rockets, coming to the conclusion that only localized effects were possible, promptly removed by atmospheric recirculation. According to the launch

*Associate Professor, Dept. Aerospace Science and Technology, 34 Via La Masa, filippo.maggi@polimi.it, AIAA Senior Member.
†Post-doctoral Research Fellow, Dept. Aerospace Science and Technology, 34 Via La Masa, AIAA Member
‡Scientific Researcher, Supersonic and Hypersonic Technologies Department, Linder Hohe.
§Head, Supersonic and Hypersonic Technologies Department, Linder Hohe.
¶Scientist, Department of Energetic Materials.
‖Deputy Director, Department of Energetic Materials,AIAA Senior Member.
**Flight Vehicle & Aerothermodynamics Engineering Section (TEC-MPA), Keplerlaan 1.
††Flight Vehicle & Aerothermodynamics Engineering Section (TEC-MPA), Keplerlaan 1.

baseline activity of that decade (some tens of large rockets per year), global hazards for climate change were not foreseen. Some open issues were still unresolved, though. The chemicals exhausted in the plume are different from the ones computed through equilibrium computation and the interaction with stratospheric conditions leads to post-combustion phenomena. In addition, heterogeneous reactions involving particulate (when present), atmosphere, and plume content have been considered important aspects for the analysis of ozone depletion and radiative forcing [1–3]. Despite the impact of a single launch is minimal compared to other manned activities, the perspectives of a strengthening space economy is rising the concerns about real environmental effects of repeated launches with increasing rates from same locations (space ports).

Solid rocket boosters of heavy launchers are powered by metalized propellants. Typically micrometric aluminum powders are used. From the ideal viewpoint, the addition of this metal fuel improves gravimetric and volumetric specific impulse. The adiabatic flame temperature increases along with the molar mass of the exhaust products. Thermodynamics predicts that a typical composition made by 68 % of ammonium perchlorate, 18 % of aluminum, and 14 % of polybutadiene binder burning at 7 MPa produces a temperature of 3404 K in the combustion chamber. After expansion ratio of 10, about 287 s of vacuum specific impulse is granted. The exhaust plume contains 34 % by mass of aluminum oxide, in solid form, and 21 % of hydrogen chloride, which turns into hydrochloric acid once in contact with atmospheric moisture (NASA CEA [4]). The physical properties of the particles (i.e. size distribution and shape) can be obtained through collection. the harsh environment represented by hot, supersonic, and reacting plume makes the task complex. In the frame of the EMAP (Experimental Modeling of Alumina Particulate in Solid Rocket Boosters) ESA-TRP program the Space Propulsion Laboratory of Politecnico di Milano (SPLab-POLIMI) has developed a probe for the collection of condensed combustion products directly at the nozzle exit. This paper describes the methodology conceived to collect solid particles inside the plume of a rocket motor and presents the results obtained in this experimental campaign. In the following, the reader will find a literature survey on the condensed combustion products in Section III, the details of the collection technique and of its implementation in Section IV, and the experimental results in Section V, followed by conclusions in Section VI.

III. Literature survey

In the past decades great effort was put for the collection of combustion products in the vicinity of the burning surface. Such practice can be performed by burning propellant strands in quench bombs. The incipient formation of metal agglomerates after the release from the propellant can be characterized. However, in a real motor the condensed particles experience a variety of phenomena while they are carried through the nozzle by the gaseous mixture. In the convergent portion of the duct the streamlines tend to cross each other and agglomerates merge, incrementing their average size. The maximum acceleration of the gas occurs at the throat. Here the velocity gradient can be so high that the critical Weber number of the liquid droplets is reached, leading to particle breakup. The condensed combustion residues eventually enter the divergent portion of the nozzle, where coalescence due to impacts prevails. Both kinetic and thermal inertia are functions of the particle size, which changes significantly through the nozzle. That is, the morphology of the agglomerates at the burning surface is not sufficient to fully understand their effect on the rocket motor performance.

A. Condensed combustion products

The condensed products contained in the rocket plume are direct consequence of the complex combustion phenomena involving aluminum throughout a sequence of physical and chemical transformations. In the first step the incipient agglomeration can be observed, consisting in aggregation-to-agglomeration processes occurring at the burning surface. Metal particles emerge at the burning surface and group into irregular shapes that protrude towards the gas phase. After inflammation, these heaps collapse into drops which detach from the propellant surface and enter the core flow [5]. High-speed and high-magnification videos show metal drops capped by some fraction of oxide, surrounded by a combustion plume. The scale of this process is in the order of few tens to some hundreds of micrometers and it is influenced by the composition, the burning pressure, and the microstructure of the propellant [6, 7]. The second step consists in the combustion of the metal inside the flow of the rocket. The liquid metal drops leaving the burning surface enter the main flow and undergo axial acceleration. Subsonic conditions are present but studies predict possible droplet break-up, depending on local core flow conditions [8]. During this phase the aluminum contained in the agglomerates progressively evaporates and is oxidized mainly by reaction with oxygen, water, and carbon dioxide [9]. Diffusion flame is produced around the drop, consuming the entire metal content if enough residence time is granted. Multimodal particle distribution of condensed combustion products (CCP) covering from sub-micrometric range (smoke oxide

particles, SOP) up to some tens of microns (agglomerates) is generated [10]. The third step consists in the evolution of the metal droplets within the accelerated flow of the nozzle. A relative velocity is generated between gas and particles. The Weber number of particles rapidly increases in the proximity of the nozzle throat, reaching the critical limit for breakup [11, 12]. Turbulent mixing and differential velocity between particles of different size can also generate the conditions for growth due to collision in the convergent part [13, 14]. Hermsen presented a global database of particles collected from nozzle exit. Several correlations were developed, though featured by low fitting quality, due to the complexity of intermingled processes to capture through analytical formulations [15]. Other data collections were reported also in a NASA handbook specialized in solid propellant performance prediction. Particle size dependence was discussed as a function of throat area, metal loading, expansion ration and several other properties. In all the cases CCP featured a volume mean diameter lower than about 20 µm but clear trends and driving parameters were difficult to highlight and identify [16] .

B. Collection of CCP

The characterization of plume content challenges a harsh environment. Optically thick plume as well as hot and supersonic flow make both intrusive and non-intrusive methods complex. For temperature and velocity the best methods are optical and spectroscopic, rather, collection remains the best option when size, shape,and chemical content is requested. A generic intrusive probe has to survive the environment. Moreover, post-processing protocol should supply information that are representative of the probed population. In the past, one of the simplest methods to fulfill the request consisted of using impinging surfaces, such as microscope slides, exposed in the vicinity of a rocket motor [17]. Optical post-processing was conducted through microscopic counting. The authors acknowledged that the mean mass of CCPs was mainly dictated by large particles, losing part of the fine fraction. Moreover, impact with the surface could alter the morphology of collected material. In the attempt to have more representative collection, Sehgal fired a rocket fully enclosed in a tank, promoting the post-fire collection of all the exhaust products [18]. The operating rocket motor pressure was adjusted by varying the nozzle throat diameter. Dobbins and Strand extended the test methodology by changing tank size, nozzle, and aluminum content from 2 % to 20 % [19]. Scattering of collected data made the authors conclude that effects were minor under the investigated conditions.

Direct collection from the plume was performed by a probe developed by Burns [20]. The probe featured a swinging motion through the rocket exhaust thanks to a hydraulic actuator. The probe chamber was initially under vacuum and a check valve was opened by the exhaust dynamic pressure. The AFRPL (Air Force Rocket Propulsion Laboratory) developed a subsonic sampling probe consisting in a torpedo-shaped tube, placed downstream the nozzle of a BATES (ballistic test and evaluation system) motor [21]. The collection technique evolved in a supersonic version by Kessel [22]. The flow inside the inner channel was supersonic and avoided front shock. The particles were slowed down and impacted against a Millipore sub-micrometric filter at the exit of the apparatus. The capturing of particles was handled differently by Carns and co-authors [23]. They described in a patent a system to remove solid particles from the exhaust flow of solid rocket motors (scrubber) before releasing the gas into the atmosphere. Even though it was not specifically designed to collect CCPs, particle separation was attained.

IV. Analysis technique

A. Concept description and implementation

The investigation of the rocket plume content is performed through a collector and a set of analyses ensuring the characterization of particle size, shape, and chemical properties. The collector is designed to be located at the nozzle exit and merges the concept of a supersonic probe and a scrubber for particle separation [22, 23]. During the fire test the tip of the collector captures part of the plume and drives the flow across a channel where cooling and deceleration is obtained through radial injection of nitrogen. The supersonic-to-subsonic transition happens in the following divergent section, if not yet occurred. Then, the flow enters the collection chamber where a counter-flow spray captures the particles. The suspension is extracted from the probe for post processing. The design considered the nominal inlet conditions of Mach number 3.23, static temperature 2226 K, and static pressure 0.053 MPa. The conceptual block schematics is reported in Fig. 1(a). The internal structure of the collection system is reported in Fig. 1(b). A more in-depth discussion concerning the design methodology can be found in Carlotti et al. [24]. The probe has been designed to withstand about 0.5 s of direct plume exposure. In front of thee probe a tungsten shield is attached to a movable arm. The installation is supplied by the DLR team and receives the trigger by the main control loop, according to the

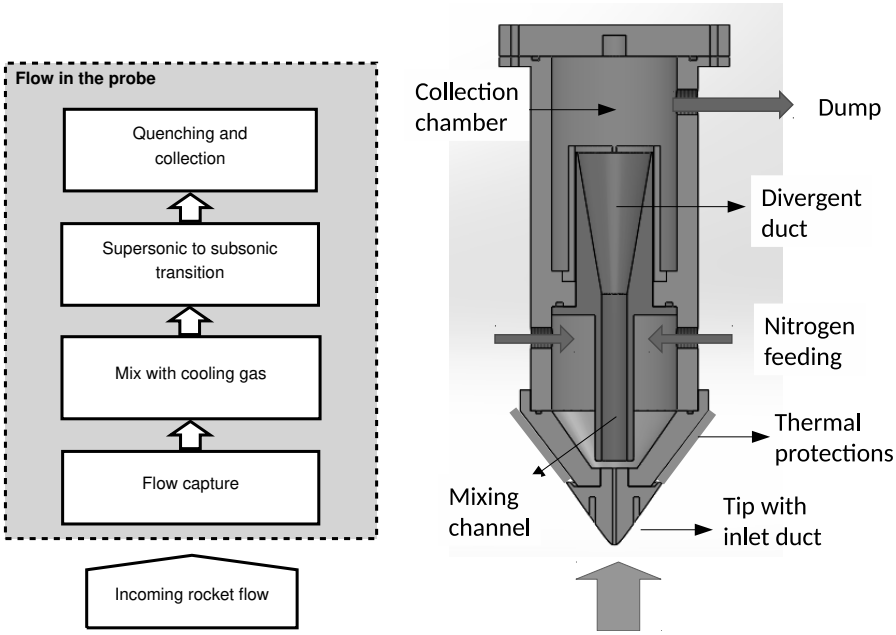

(a) Conceptual blocks of the probe (b) Internal scheme of the probe

Fig. 1 Rocket Plume Collector

pressure level of the rocket motor. The main control system identified pressure rise inside the combustion chamber and after a pre-determined delay excluding the ignition transient, quenching spray was triggered and, after about 200 ms opening command was sent to the shield, followed by closing after about 500 ms to 700 ms. The effective exposure time was influenced by inertia of the moving arm but this value was not critical for measurement. The movement of the shield is synchronized with spray of liquid in the quenching chamber. A final spray was finally released without inlet flow to clean up the collection volume. Timing of the RPC test is depicted in Fig. 3. Outermost supply lines are not protected by the shield and a silicate-based thermal paste is applied to these parts. The rocket plume collector and related setup was integrated in a vertical wind tunnel along with other different diagnostics. The integrated setup of the EMAP project is visible in Fig. 2 and a detailed discussion can be found in a recent paper by Saile and co-authors [25]. During the hot flow tests, the RPC was placed at 180 mm from the nozzle exit section because of DLR internal safety requirement and to grant free optical path to the other non-intrusive techniques. The gap was also necessary to ensure the proper movement of the tungsten thermal shield. Particles were quenched in a chlorine-based hydrocarbon liquid. Collected materials have been post processed by means of laser diffraction methodology using a Malvern Mastersizer 2000 with liquid dispersion and/or Scanning Electron Microscope (SEM). The former enables to compute the particle size distribution, the latter provides information on the morphology and confirms the size of the particles under analysis. Additionally, an XRD campaign provided information concerning the composition of the residues and the EDX technique was used for elemental analysis.

B. Lessons learned on critical components

The correct operation of the probe resides in the proper flow generation inside the internal duct, from the supersonic inlet to the spray collection. Moreover, the design and the operating procedures need to take into consideration the harsh environment of the supersonic high-enthalpy plume, where the probe is expected to operate.

Collection concept

The entire life-cycle of the particles should ensure that the collection is performed properly and the following sample handling would not alter the main parameters of the particulate. During a preliminary cold-flow test campaign the probe was tested in the VMK wind tunnel at relevant exit Mach number of 3.00 and different upstream total pressures (both nominal and off-design). The experimental assembly is shown in Fig. 4(a). The tests had a two-fold scope: on the one

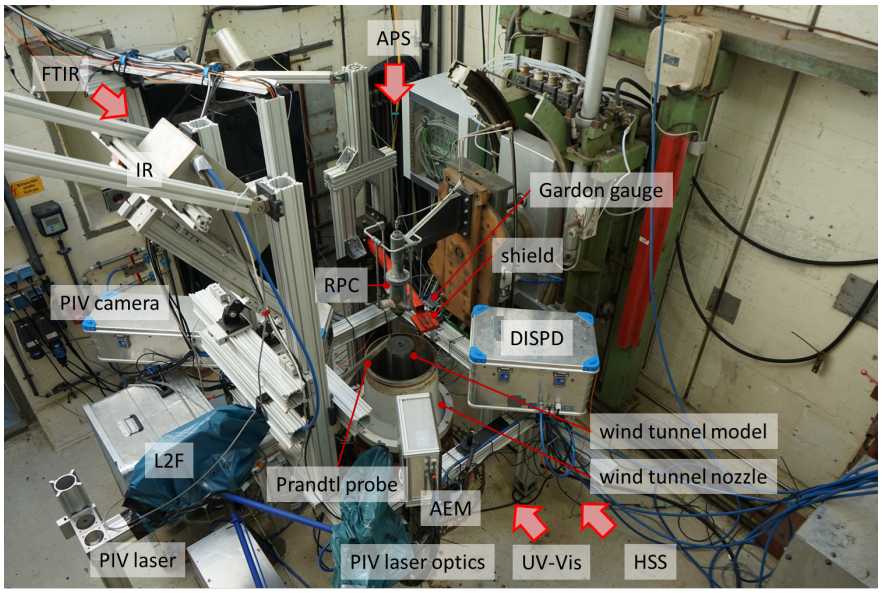

Fig. 2 Global view of the EMAP experimental setup [25]

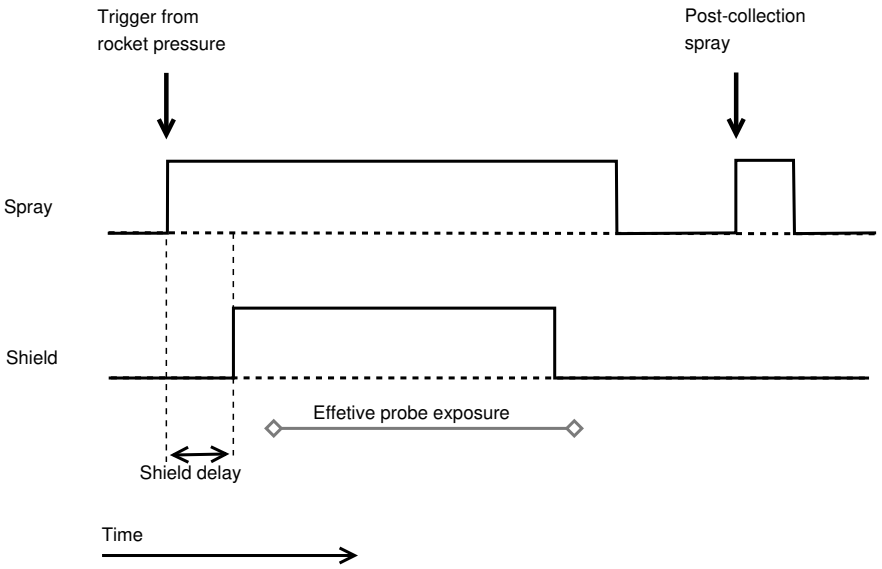

Fig. 3 Timing of the probe during hot flow tests.

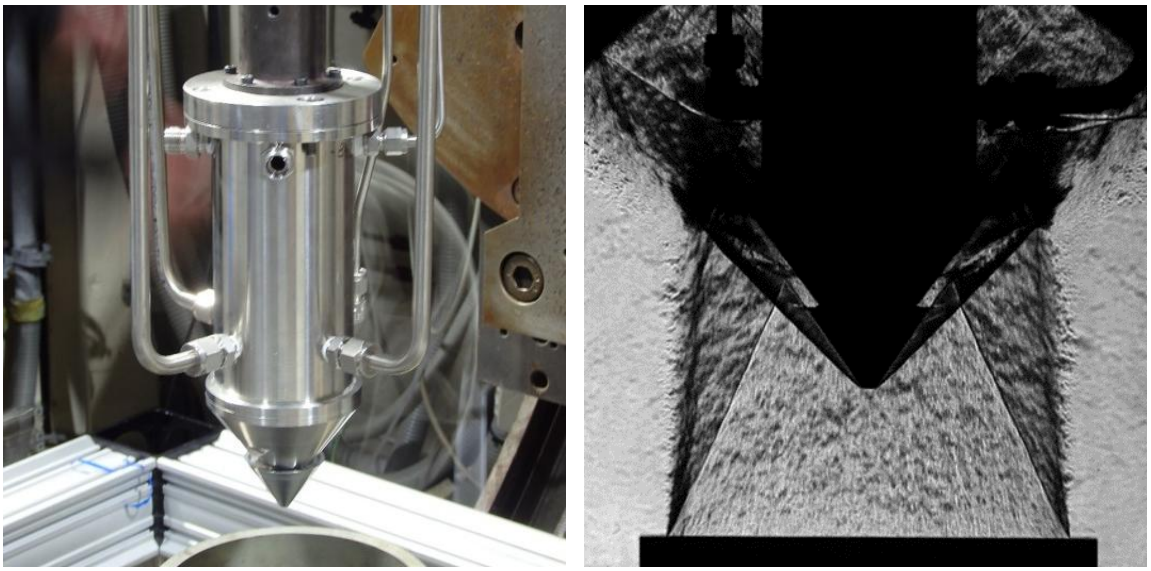

(a) Probe ready for test

(b) Schlieren visualization of a test

Fig. 4 Cold flow test campaign

Table 1 Comparison between original and collected particle diameters. Data obtained from laser diffraction analysis.

	D(3,2), [μm]	D(4,3), [μm]
original	5.693	17.032
collected	5.572	16.993

hand through Schlieren techniques the identification of bow-shock insurgence would have indicated the presence of an internal choking and improper fluid dynamic behavior, on the other hand seeding of the flow with inert particles would validate the collection methodology. During this step, water was used as capturing liquid and magnesium oxide as dispersed medium. The particles seeding the flow were sieved, obtaining a diameter range similar to the one expected in the final experimental campaign. The coolant flow was produced by nitrogen. The respective mass flow rates were adapted to the cold flow operating conditions. After the tests, particle suspensions were shipped to SPLab-POLIMI for particle size distribution (PSD) analysis through laser diffraction.

Results of the cold-flow test campaign validated the design of the probe. Schlieren visualizations captured the presence of an oblique shock at the lip of the probe ingestion point without external shocks under both design and off-design conditions, confirming the absence of choking inside the internal channel, as planned by the design (see Fig. 4(b)). Table 1 reports the comparison between original and collected particles for the nominal operating condition of the probe, confirming that the collection method is capable of capturing a representative population of the particles suspended in the supersonic flow. Data were reported for a total wind tunnel total pressure of 25 bar.

High-temperature tip

The proper capturing of the probe is ensured by the presence of sharp tip inlet, directly exposed to the hot flow. This item suffers high thermal load, strong temperature gradient, and consequent thermal shock. The design of the component was a compromise between general strength, ease of operations, ease of production, and global cost. Screw fixing was considered the best option for fast replacement during campaign. Both extruded graphite and electrographite were considered and used for prototyping. The latter one was selected because of the reduced size of internal grains, higher compactness, better machinability and absence of evident impurities. In Fig. 5 the XCT analyses of tip prototypes are reported.

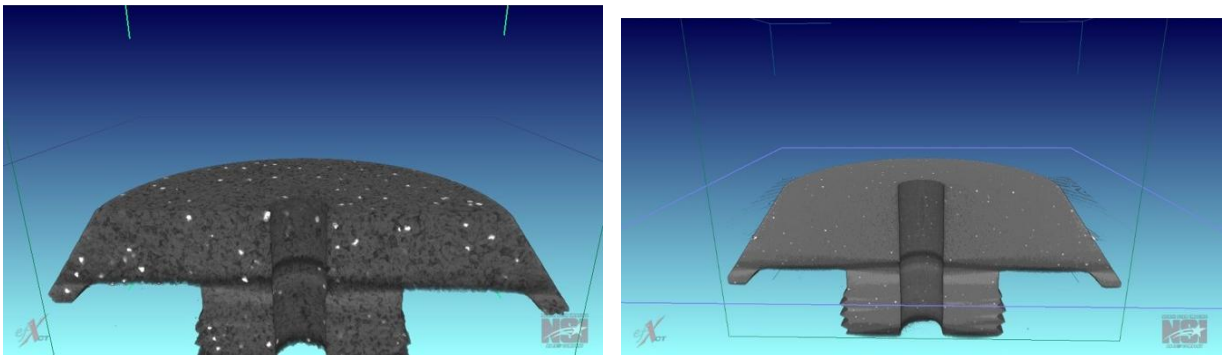

(a) Extruded, nominal grain size 800 µm (b) Electrographite, nominal grain size 7 µm

Fig. 5 Tomography of tips made by different graphite grades

At the beginning of the hot flow tests the fixture was modified because the rigid screw connection fragmented into pieces due to different thermal expansion of fragile graphite and metal. A soft glued fixture resolved the issue. After exposure, the tip demonstrates good mechanical properties. It shows accumulation of aluminum oxide on the side walls and, partially, on the sharp edge. The curvature modification did not produce modifications in collection capability. The internal channel does not show signs of wearing and is free from deposits, with the exception of a minor presence of alumina just downstream the inlet. The tomographic analysis of a used tip is reported in 6. The color scale was selected to highlight the presence of aluminum oxide at the surface (whitish color). The reader can note that the deposit is non-symmetrical because of the protective shutter movement. Visible cracks are not present.

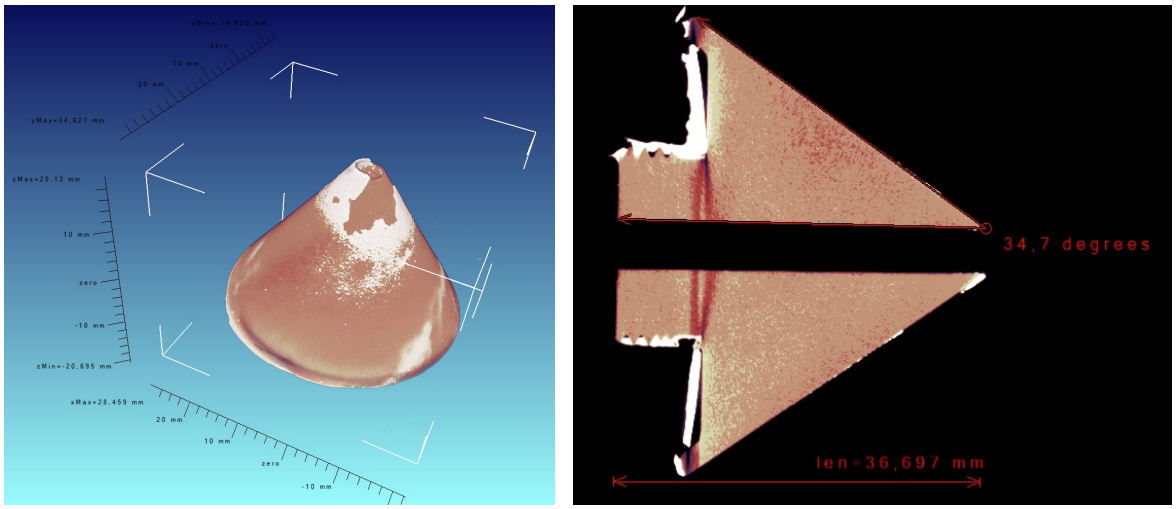

(a) 3D Reconstruction (b) Axial section

Fig. 6 Tomography of a tip after use

V. Experimental results

The collection method was applied to small scale test motors having variable nominal operating pressures, in the range 3.0 MPa to 6.0 MPa, and variable expansion ratios, between 1 to 14. The motors was loaded with an end-burning geometry, targeting a neutral pressure trace. The propellant was based on HTPB binder and ammonium perchlorate oxidizer, having either 5 % or 18 % aluminum load. Some tests have been also conducted with inert aluminum oxide

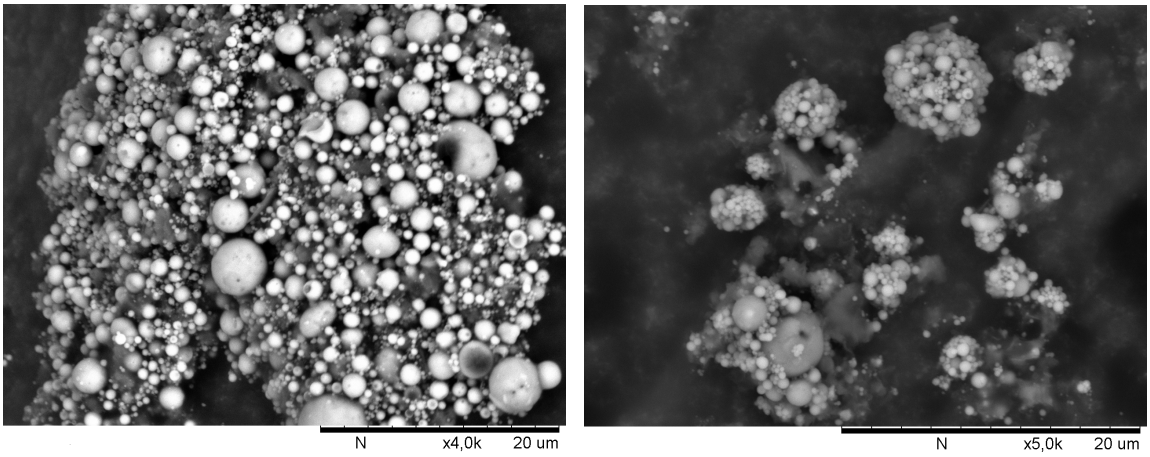

(a) (b)

Fig. 7 SEM images of collected particles

particles for preliminary tests.

The procedure implemented in the rocket plume collector suspends the particles in a halogen-based quenching liquid. After the test, the probe is dismounted and the liquid medium is removed with a pipette to extract the particles. Then, the sample is washed and with acetone and centrifuged multiple times to remove the original liquid. Finally the particles are dried overnight inside an oven and are shipped for analysis to SPLab-POLIMI in powdered form.

Before the analysis, it is necessary to re-suspend the sample in a carrier. This step is quite delicate because the procedure should ensure the dispersion of the particles without losing part of it. Ultrasound treatment and, in case of PSD analysis, Igepal dispersion agent have been used. After this procedure, a complete characterization of the particles is obtained. Morphology, particle shape and surface finishing can be obtained by qualitative observations through scanning electron microscopy (SEM); the particle size distribution and the relevant properties (mass-mean diameters, surface-mean diameters, percentiles) are obtained through laser diffraction technique, the crystalline nature of the sample is investigated through X-ray Diffraction analysis (XRD); the surface chemical composition is obtained through Energy Dispersive X-ray analysis (EDX).

Finally, the deposition of the liquid aluminum/alumina film layer in the nozzle convergent section of one test has been extracted and analyzed. In this case, tomographic X-ray inspection and XRD analysis were performed for identification of the crystalline form created during the deposition.

A. Morphology Characterization

SEM pictures were obtained by a Hitachi TM 3000 scanning electron microscope at 15 kV and several magnifications. Prior the test, ultrasonic bath procedure was used to enhance the dispersion of the powders. Then, a fixed amount of sample was dispersed on a SEM sample holder using a pipette. Images can be taken after the solvent was evaporated. The particles visible in Fig. 7 are mainly spherical and range from 0.1 µm to 6.0 µm diameter, the large majority being fine particles, between 0.1 µm to 2.0 µm. The surface is smooth. Images reveal systematic presence of large fractured hollow particles (diameter $\geq$ 2 µm).

B. Particle size

The amount of collected particles, in the range of about 200 milligrams, and the accuracy of the measurement suggested the way of liquid dispersion a[illegible]aser diffraction analysis to recover the PSD. Malvern Mastersizer 2000 instrument with Hydro unit was employed The preparation of the sample is fundamental in this kind of test as separation of particles should be ensured for the measure. The particles were suspended in bidistilled water once received with a series of ultrasound treatments and dispersion agents both before and during the measure. The timing between the ultrasound bombardment and the measure also was important as the particles tend to aggregate as time passes, even under vigorous stirring. Multiple scattering phenomena were also observed during the post process. Figure 8 reports

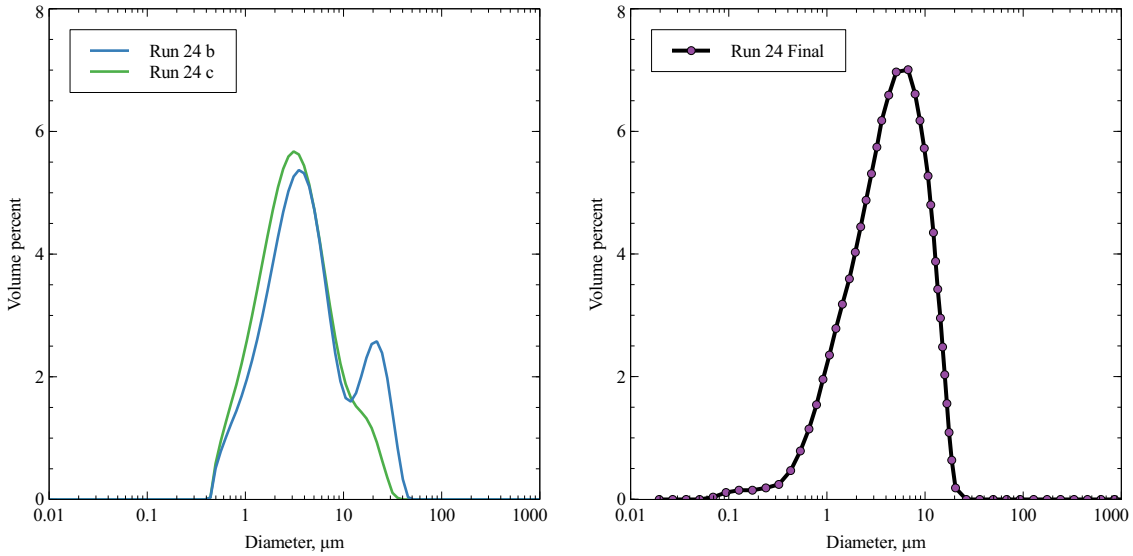

(a) Before complete treatment

(b) Complete sample treatment

Fig. 8 PSD of collected particles

a series of measurements taken during the tuning of the analysis procedure. The reader can notice that inaccurate pre-treatment caused the generation of spurious peaks or shoulders in the curves reported in Fig. 8(a) whereas the sample revealed a purely monomodal dispersion, once the analysis procedure was assessed.

The reported tests are referred to the Run number 24. The effective chamber pressure during the particle siz collection was 6.2 MPa and the exposure time was about 0.5 s to 0.7 s. The propellant in the motor was made by HTPB (14 % by mass), ammonium perchlorate (56.1 % coarse fraction, 24.4 % fine jet-milled fraction), hematite iron oxide (0.5 %), and aluminum (5 %, Alpoco Type II, nominal size between 12 µm to 18 µm). The expansion ratio was 14 a nominal exit Mach number of 3.23.

The monomodal particle size distribution peaks between 5 µm to 8 µm with a part in the sub-micrometric range. The volume-mean particle size is 5.3 µm, the surface-mean diameter is 2.2 µm while the percentiles d(0.1)/d(0.5)/d(0.9) are respectively 1.10/4.36/11.1µm, with a span of 2.29. The resulting number is in line with the data reported for particle sizes available in ref. [16].

C. Chemical composition

D. X-ray diffraction analysis

The tests were executed by a PANalytical X'Pert alpha-1 Θ/2Θ X-Ray Diffractometer with Bragg Brentano geometry. The limited amount of material required the use of a zero-background sample holder. The beam diffracts through the crystal and the signal was collected by a detector at different angles of diffraction. The diffraction pattern of one sample is ported in Fig. 9. The black curve reports on the vertical axis the intensity of diffracted signal as a function of the different angles (horizontal axis). The vertical color bars show the ideal pattern of the crystalline structures identified during the post-processing phase. The analysis identifies two main crystalline forms of aluminum oxide: $\gamma - Al_2O_3$ and $\alpha - Al_2O_3$. Graphite is also found. The presence of graphite can be attributed either to some wearing of the tip or to the carbon generated during the incomplete combustion of the binder. Graphite time scale formation should be verified as the binder is prone to soot generation, being an HTPB. It is known from the literature that the decomposition of the polymer under rapid heating conditions generates butadiene and vinyl-cyclo-hexene, which can be precursors of soot. Moreover, composite propellants locally present a diffusive flame which can favor the generation of fuel-rich thin layers and, thus, favor the local incomplete carbon oxidation. Aluminum oxide derives from the combustion of aluminum in the combustion chamber. Aluminum oxide melts at about 2300 K so in the combustion chamber they are in liquid form. During the expansion the particles expand and cool down by convection with the surrounding gas medium.

Some radiation loss is also present towards the nozzle walls. The Al_2O_3 particles are expected to be in solid form once they leave the nozzle and enter the probe. The α and the γ phases are two polymorphic forms of solid alumina. The former one (corundum, trigonal) is the stablest condition while the latter one is a transition (metastable) cubic form. Different paths lead to the formation of γ and α, starting from intermediates, molten or vapor phase [26]. Literature reports that $\gamma \rightarrow \alpha$ conversion is mostly indirect and passes through the nucleation of the final phase. On this point the literature is contradictory. A review by Levin does not report direct paths while Steiner and co-authors show a study on the kinetics of $\gamma \rightarrow \alpha$ conversion [27]. The latter research does not give a concluding view of the conversion mechanism and underlines that the observed kinetics may be the result lf [illegible] complex pathways. The study shows a very sharp increment in reaction rate with the temperature but the study investigates a temperature range up to 1473 K and the time scales are in the order of some minutes. Thus, at the author's knowledge the $\gamma \rightarrow \alpha$ conversion does not seem compatible with the residence times of alumina droplets. Another study by Ishizuka and co-authors [28] clearly reports that rapid cooling of melts or vapor condensation form preferably metastable alumina phases (such as the γ one) whereas no evidence of α formation from condensation is found in the literature. It seems possible that the two alumina kinds are derived from different paths.

It is interesting to note that the deposition of alumina inside the nozzle could also be observed and analyzed. During the experimental tests the clogging of the convergent part of the gas dynamic nozzle was identified in different runs. The occurrence mainly happened in the firings characterized by propellants with low aluminum loading, probably because solid particles sick to the walls due to lower temperature with respect to a combustion with heavy propellant aluminization. A melt layer is generated internally and reduces progressively the passage area, often resulting in nozzle throat reduction and release of large slivers from the nozzle that detach due to gas dynamic effect from the deposited liquid layer. The collection tests performed by the probe were exempt from this issue because the overall control loop activated the collection early in the firing, before the clogging effect was identified in the pressure traces, as visible in Fig. 10.

At the end of firing RUN026-V38-END the clogging of the convergent was preserved and analyzed through X-ray computed microtomography and an XRD analysis. The original sample is reported in Fig. 11.

The X-ray tomography was performed at the Advanced Manufacturing Laboratory of Politecnico di Milano (AMALA) using a X-25 micro-tomographic machine produced by NSI and equipped with an X-ray gun capable of up to 160 kV acceleration. The instrument is metrically certified [29]. The measurement was performed using the NSI proprietary software *eX-View*. The 3D reconstruction is reported in Fig. 12, the longitudinal cuts are shown in Fig. 13 and the cross sections are reported in 14.

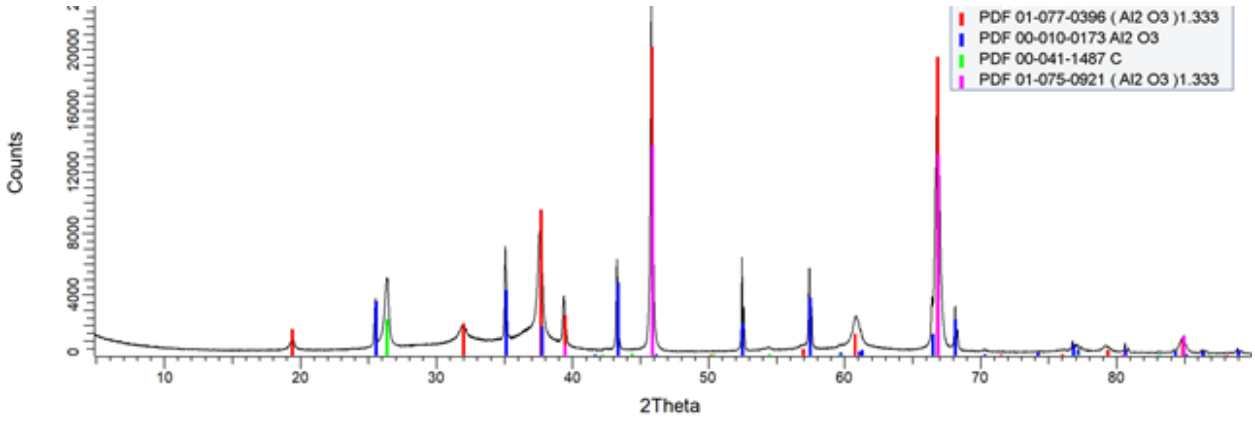

Fig. 9 X-ray diffraction pattern of samples from RUN030

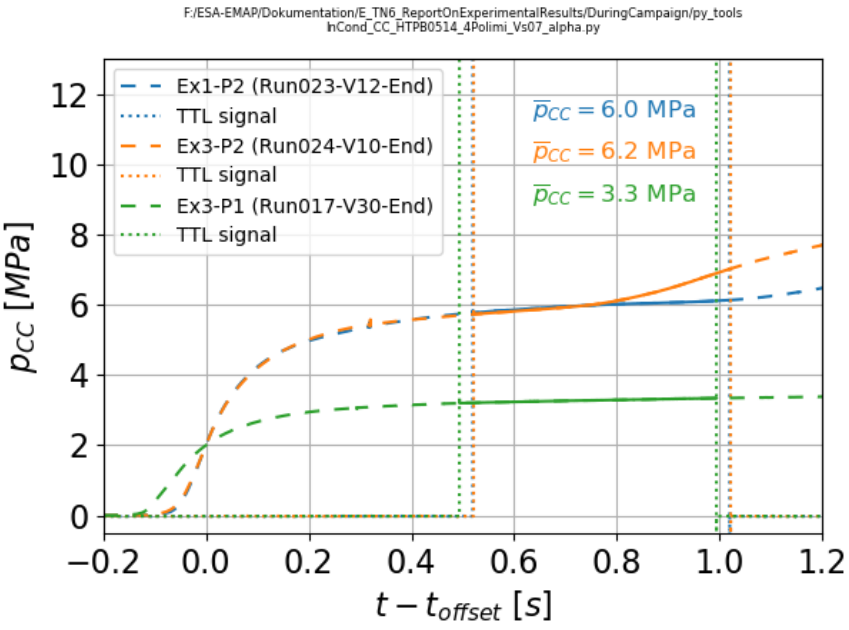

Fig. 10 Pressure trace of different runs and probe activation timing

Fig. 11 Nozzle clogging of run 026-V38-END (convergent).

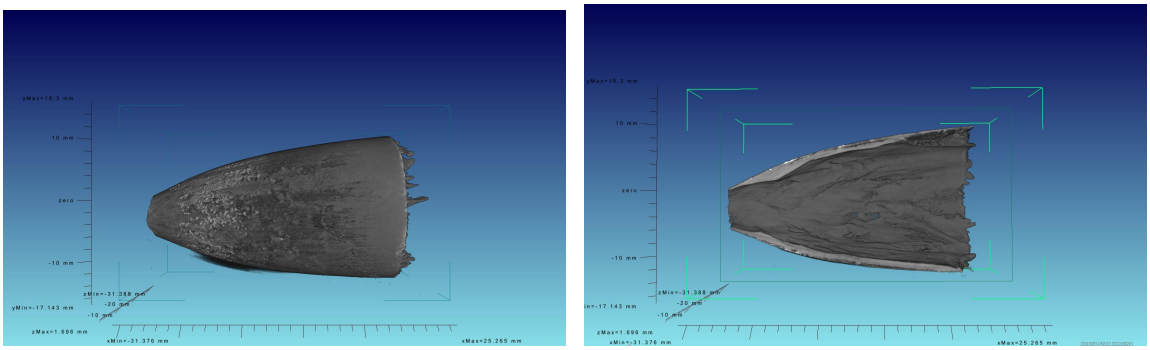

(a) (b)

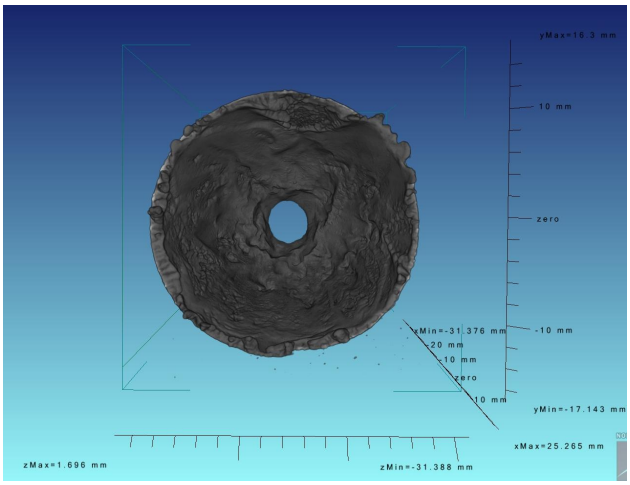

(c)

Fig. 12 Reconstruction of XCT scan

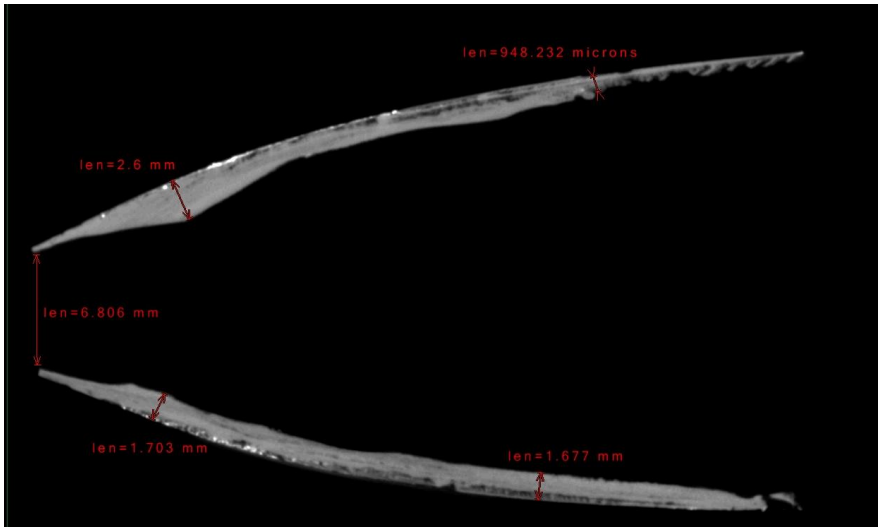

Fig. 13 Axial cut from XCT reconstruction

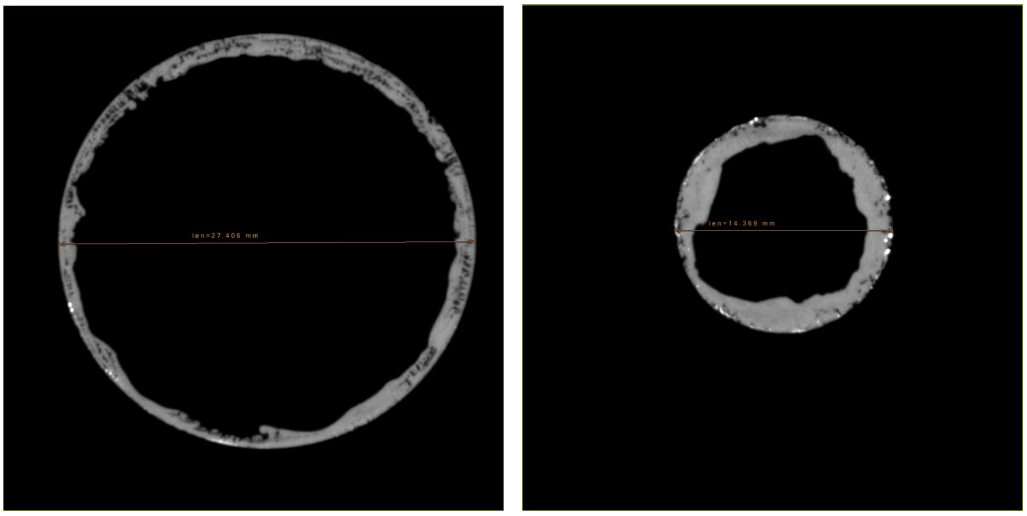

(a) Inlet side (b) Throat proximity

Fig. 14 Cross sections of nozzle (convergent) deposition at different expansion ratios

The figures show the non uniform profile of the deposition inside the nozzle. The thickness grows progressively along the axis and reaches a maximum before the throat. The shaping is due to internal fluid dynamic forces interacting with the liquid molten layer of aluminum oxide. The deposition is partially porous and small vacuoles are located close to the wall.

A sample was removed from the convergent-side edge, powdered, and analyzed through XRD. The measurement identified the presence of *alpha* aluminum oxide, only. It is known that the layer is mainly formed by impact of molten agglomerates with the convergent. In this last case, the cooling occurred inside a combustion chamber, granting longer time scales. It is not clear the reason of the porosity at the convergent side edge. The combustion chamber temperature would enable the boiling of metal aluminum which deposited in the early phase of the firing at the wall but this point is still a hypothesis.

VI. Conclusions

The paper has presented a methodology for the analysis of solid propellant condensed combustion products, probing the samples from the plume of a rocket motor. The method involved design and implementation of a new supersonic probe and precise definition of post-collection protocols for analysis. The scope of the probe was to sample a representative quantity and quality of particles from the plume. Validation of the collection concept was conducted in cold-flow conditions. The hot flow test collection enabled the complete characterization of the plume content. In the case described in the paper, particles exiting from the nozzle have a mean diameter of about 5 µm and are mostly concentrated in the range 1 µm to 10 µm. The composition showed that aluminum is fully burnt and that two types of solid aluminum oxide (α and γ forms) are present in the suspended medium. SEM analyses show that particles have smooth surface.

The analysis methodology described in this paper represents a valid instrument for reliable characterization of rocket plume content, at the exit of the nozzle. These pieces of information represent the final condition of the agglomerate evolution inside the rocket motor. These data sets can be used inside models for environmental impact prediction with real and dedicated data. Moreover, the same data can be used to tune up and validate the prediction capability of models for internal multiphase evolution and metal combustion.

Concept and post-processing procedure demonstrated adequate robustness for characterization of small-scale rocket motor exhaust and can be extended to larger scale, with some architectural modifications. As a matter of critical components, use of tungsten or other high-temperature metal, in spite of graphite, may be preferable for tip production. Despite minimal contamination of the sample from graphite erosion, mechanical strength may be improved. Shielding methodology is adequate for current application but should be redesigned, in case of scale-up.

Acknowledgments

The authors acknowledge the financial support of the European Space Agency through the contract No. 4000114698/15/Nl/SFe. The authors also acknowledge the work of Dr. Gianluigi Marra from ENI Donegani Institute and the cooperation with the Advanced Manufacturing Laboratory (AMALA) of Politecnico di Milano.

References

[1] Ross, M., Mills, M., and Toohey, D., "Potential climate impact of black carbon emitted by rockets," *Geophysical Research Letters*, Vol. 37, No. 24, 2010. https://doi.org/10.1029/2010gl044548.

[2] Solomon, S., "Stratospheric Ozone depletion: a review of concepts and history," *Reviews of Geophysics*, Vol. 37, No. 3, 1999, pp. 275–316.

[3] Hawks, C. W., "Environmental effects of solid rocket propellants, perceptions and realities," *Environmental Aspects of Rocket and Gun Propellants*, AGARD Conference Proceedings, Vol. AGARD-CP-559, NATO, 1995.

[4] Gordon, S., and McBride, B. S., "Computer Program for Calculation of Complex Chemical Equilibrium Compositions and Applications," Tech. Rep. RP-1311, NASA Reference Publication, 1994.

[5] Price, E. W., "Combustion of metallized propellants," *Fundamental of Solid Propellant Combustion*, Progress in Astronautics and Aeronautics Series, Vol. 90, edited by K. K. Kuo and M. Summerfield, AIAA, New York, NY, USA, 1984, pp. 479–513.

[6] DeLuca, L., Galfetti, L., Colombo, G., Maggi, F., Bandera, A., Babuk, V. A., and Sinditskii, V. P., "Microstructure effects in aluminized solid rocket propellants," Vol. 26, No. 4, 2010, pp. 724–733. https://doi.org/10.2514/1.45262.

[7] Maggi, F., DeLuca, L. T., and Bandera, A., "Pocket Model for Aluminum Agglomeration Based on Propellant Microstructure," *AIAA Journal*, Vol. 53, No. 11, 2015, pp. 3395–3403. https://doi.org/10.2514/1.j053992.

[8] Maggi, F., Dossi, S., and DeLuca, L. T., "Combustion of metal agglomerates in a solid rocket core flow," *Acta Astronautica*, Vol. 92, No. 0, 2012, pp. 163–171. https://doi.org/10.1016/j.actaastro.2012.04.036.

[9] Beckstead, M. W., "A summary of aluminum combustion," RTO-EN 023, NATO, 2002.

[10] Babuk, V. A., "Problems in studying formation of smoke oxide particles in combustion of aluminized solid propellants," *Combustion, Explosion, and Shock Waves*, Vol. 43, No. 1, 2007, pp. 38–45.

[11] Caveny, L. H., and Gany, A., "Breakup of Al/Al_2O_3 Agglomerates in Accelerating Flowfields," *AIAA Journal*, Vol. 17, No. 12, 1979, pp. 1368–1371. https://doi.org/10.2514/3.7633, URL http://dx.doi.org/10.2514/3.7633.

[12] Gany, A., Caveny, L. H., and Summerfield, M., "Aluminized solid propellants burning in a rocket motor flowfield," *AIAA Journal*, Vol. 16, No. 7, 1978, pp. 736–739. URL http://arc.aiaa.org/doi/pdf/10.2514/3.60959.

[13] Marble, F. E., "Droplet agglomeration in rocket nozzles caused by particle slip and collision," *Astronautica Acta*, Vol. 13, No. 2, 1967, pp. 159–166.

[14] Crowe, C. T., and Willoughby, P. G., "A study of particle growth in a rocket nozzle." *AIAA Journal*, Vol. 5, No. 7, 1967, pp. 1300–1304.

[15] Hermsen, R. W., "Aluminum oxide particle size for solid rocket motor performance prediction," *Journal of Spacecraft and Rockets*, Vol. 18, No. 6, 1981, pp. 483–490.

[16] AA.VV., "Solid Rocket Motor Performance Analysis and Prediction," Tech. Rep. SP-8039, NASA, May 1971.

[17] Brown, B., and McArty, K. P., "Particle size of condensed oxides from combustion of metalized solid propellants," *Symposium (International) on Combustion*, Vol. 8, Elsevier, 1961, pp. 814–823.

[18] Sehgal, R., "An experimental investigation of a gas-particle system." Tech. Rep. DTIC Accession Number AD0274314, Jet Propulsion Laboratory, 1962.

[19] Dobbins, R. A., and Strand, L. D., "A comparison of two methods of measuring particle size of Al2O3 produced by a small rocket motor," *AIAA Journal*, Vol. 8, No. 9, 1970, pp. 1544–1550. https://doi.org/10.2514/3.5945.

[20] Burns, E. A., "Analysis of MINUTEMAN exhaust products," Tech. Rep. DTIC Accession Number AD 432233, Aerojet General Corporation, 1962.

[21] Misener, J. A., et al., "Exhaust plume measurements fo 15-pound BATES Motors," Tech. Rep. AFRPL TR-85-013, Air Force Rocket Propulsion Laboratory, 1985.

[22] Kessel, P. A., "Rocket exhaust probe," , 1987. US Patent 4,662,216.

[23] Carns, R. H., et al., "Rocket motor exhaust scrubber," , 2005. US Patent 6,964,699 B1.

[24] Carlotti, S., Maggi, F., Ferreri, A., Galfetti, L., Bisin, R., Saile, D., Gülhan, A., Groll, C., and Langener, T., "Development of an intrusive technique for particle collection in rockets plume," *Acta Astronautica*, Vol. 158, 2019, pp. 361–374.

[25] Saile, D., Kühl, V., Willert, C., Liljedahl, M., Wingborg, N., Carlotti, S., Maggi, F., van den Eynde, J., Langener, T., and Gülhan, A., "Overview to the ESA-EMAP Project: Characterization of SRM Plumes with Alumina Particulate in Subscale Testing," *International Conference on Flight Vehicles, Aerothermodynamics and Re-Entry Missions & Engineering*, 2019. Monopoli, Italy.

[26] Levin, I., and Brandon, D., "Metastable Alumina Polymorphs: Crystal Structures and Transition Sequences," *Journal of the American Ceramic Society*, Vol. 81, No. 8, 2005, pp. 1995–2012. https://doi.org/10.1111/j.1151-2916.1998.tb02581.x.

[27] Steiner, C. J.-P., Hasselman, D. P. H., and Spriggs, R. M., "Kinetics of the Gamma-to-Alpha Alumina Phase Transformation," *Journal of the American Ceramic Society*, Vol. 54, No. 8, 1971, pp. 412–413. https://doi.org/10.1111/j.1151-2916.1971.tb12335.x.

[28] Ishizuka, S., Kimura, Y., Yamazaki, T., Hama, T., Watanabe, N., and Kouchi, A., "Two-Step Process in Homogeneous Nucleation of Alumina in Supersaturated Vapor," *Chemistry of Materials*, Vol. 28, No. 23, 2016, pp. 8732–8741. https://doi.org/10.1021/acs.chemmater.6b04061.

[29] Moroni, G., and Petrò, S., "A Discussion on Performance Verification of 3D X-ray Computed Tomography Systems," *Procedia CIRP*, Vol. 75, 2018, pp. 125–130. https://doi.org/10.1016/j.procir.2018.04.064.